Solution Structure of Domain 6 from a Self-Splicing Group II Intron Ribozyme: A Mg2+ Binding Site is Located Close to the Stacked Branch Adenosine

Erat, M C ; Zerbe, O ; Fox, T ; Sigel, Roland K O

Abstract: Group II intron self-splicing is essential for correct expression of organellar genes in plants, fungi, and yeast, as well as of bacterial genes. Self-excision of these autocatalytic introns from the primary RNA transcript is achieved in a two-step mechanism apparently analogous to the one of the eukaryotic spliceosome. The 2'-OH of a conserved adenosine (the branch point) located within domain 6 (D6) acts as the nucleophile in the first step of splicing. Despite the biological importance of group II introns, little is known about their structural organization and usage of metal ions in catalysis. Here we report the first solution structure of a catalytically active D6 construct encompassing the branch point and the neighboring helical regions from the mitochondrial yeast intron ai5 . The branch adenosine is the single unpaired nucleotide, and, in contrast to the spliceosomal branch site, resides within the helix being partially stacked between the two flanking GU wobble pairs. We identified a novel prominent Mg2+ binding site in the major groove of the branch site. Importantly, Mg2+ addition does not impair stacking of the branch-adenosine, but in contrast rather strengthens the interaction with the flanking uridines, as shown by NMR- and fluorescence studies. This means, that domain 6 presents the branch adenosine in a stacked fashion to the core of group II introns upon folding to the active conformation.

DOI: https://doi.org/10.1002/cbic.200600459

A Mg^{2+} Binding Site is Located in Close Neighborhood to the Stacked Branch-Adenosine in Domain 6 of a Self-Splicing Group II Intron Ribozyme[**]

Michèle C. Erat,[a] Oliver Zerbe,[b] Thomas Fox,[a] and Roland K. O. Sigel*[a]

Running titles: (a) Domain 6 of a Group II Intron Ribozyme
(b) M. C. Erat et al.

[a] Prof. Dr. R. K. O. Sigel, Michèle C. Erat, Dr. T. Fox
Institute of Inorganic Chemistry, University of Zürich
Winterthurerstrasse 190
CH-8057 Zürich (Switzerland)
Fax: ++41-44-635 6802
Email: Roland.Sigel@aci.unizh.ch

[b] PD Dr. O. Zerbe
Institute of Organic Chemistry, University of Zürich
Winterthurerstrasse 190
CH-8057 Zürich (Switzerland)

(footnote to first page)

[**] Abbreviations and definitions: ai5γ, yeast mitochondrial group II selfsplicing intron in the cytochrome c oxidase subunit 1 (Sc.cox1/5 intron); CMCT, 1-cyclohexyl-3-(2-morpholinoethyl) carbodiimide metho-*p*-toluene sulfonate; COSY, correlated spectroscopy; D56, domains 5 and 6; D6, domain 6; EDTA, ethylenediamine-N,N,N',N'-tetraacetic acid disodium salt; HSQC, heteronuclear single quantum coherence; LINE elements, long interspersed elements; NMR, nuclear magnetic resonance; NOE, nuclear overhauser effect; NOESY, nuclear overhauser effect spectroscopy; NTP, nucleoside 5'-triphosphate; ppm, parts per million; r.m.s.d., root-mean-square deviation; snRNA, small nuclear ribonucleic acid; TOCSY, total correlation spectroscopy; wt, wild type.

Abstract: Group II intron self-splicing is essential for correct expression of organellar genes in plants, fungi, and yeast, as well as of bacterial genes. Self-excision of these autocatalytic introns from the primary RNA transcript is achieved in a two-step mechanism apparently analogous to the one of the eukaryotic spliceosome. The 2'-OH of a conserved adenosine (the branch point) located within domain 6 (D6) acts as the nucleophile in the first step of splicing. Despite the biological importance of group II introns, little is known about their structural organization and usage of metal ions in catalysis. Here we report the first solution structure of a catalytically active D6 construct encompassing the branch point and the neighboring helical regions from the mitochondrial yeast intron ai5γ. The branch adenosine is the single unpaired nucleotide, and, in contrast to the spliceosomal branch site, resides within the helix being partially stacked between the two flanking GU wobble pairs. We identified a novel prominent Mg^{2+} binding site in the major groove of the branch site. Importantly, Mg^{2+} addition does not impair stacking of the branch-adenosine, but in contrast rather strengthens the interaction with the flanking uridines, as shown by NMR- and fluorescence studies. This means, that domain 6 presents the branch adenosine in a stacked fashion to the core of group II introns upon folding to the active conformation.

Keywords: bioinorganic chemistry • RNA, ribozymes • group II intron • splicing, branching • NMR

Introduction

Group II introns are self-splicing ribozymes found in organellar genes in plants, fungi, and yeast, as well as in bacterial genomes.[1] Some group II introns also encode for a maturase protein, enabling these RNAs to act as mobile genetic elements.[1] Although their direct occurrence is nowadays confined to a limited range of organisms, these catalytic RNAs may have played an important role in evolution. Taking into account related nuclear introns and transposable LINE elements, as much as one third of the human DNA may have evolved from ancestral group II introns.[2] In addition, based on reaction pathway and sequence similarity, a common ancestry with the eukaryotic spliceosomal machinery has been proposed.[1] The spliceosome is a multicomponent RNA-protein complex that occurs in higher eukaryotes and consists of five highly structured snRNAs (U1, U2, U4, U5 and U6) and numerous proteins, the latter ones presumably having structural roles.[3,4] Here, splicing occurs through the assembly of the snRNAs at pre-mRNA splice sites thereby exhibiting a mechanism that is very similar to the one found for group II introns. It is surprising that despite the evident biological importance of group II introns, only little is known about their structural organization[5-7] and the involvement of metal ions in catalysis.[8]

Group II introns share a common secondary structure of six domains. The catalytic core is constituted of nucleotides from domains 1, 5, 6, the linker region between domains 2 and 3 as well as the splice site itself.[7] In parallel to the spliceosome, the 2'-OH of a conserved adenosine, which in group II introns is located within domain 6, serves as the attacking nucleophile in the first step of splicing. This leads to the formation of a 2',5'-phosphodiester linkage and the subsequent excision of the intron in form of a lariat, analogous to the spliceosome. Obviously the positioning of the 2'-OH of the branch-point A is of paramount importance for correlating structure and function in both systems. However, the base pairing pattern and geometrical conformation of the branch adenosine in group II intron splicing has been a matter of debate. Secondary structure alignments and phylogenetic comparisons predict the branch A to form a single-nucleotide bulge, as it is also the case in the spliceosome.[9,10] Instead, the recent crystal structure of a D56 construct shows a shifted base pairing pattern and a two-nucleotide bulge.[5] To clarify the base pairing geometry in D6 and view the structural features of the branch A we have now solved the solution structure of this region by NMR.

It is indisputable that metal ions are always interwoven with RNA structure and function.[11-13] All group II introns that have been investigated to date require divalent metal ions for folding and catalysis.[8,14,15] Hydrolytic cleavage-[16] and sulfur-substitution experiments,[17] as well as investigations by NMR[6] and X-ray[5] confirmed metal ion binding to domain 5 and other parts of the catalytic core. Concerning the branch domain 6, metal ion binding to the minor

groove of the branch region was detected by Tb^{3+} cleavage experiments.[16] In addition, the crystal structure of a permuted D56 construct shows a cobalt(III)hexammine binding site near the two-nucleotide bulge.[5] However, $Co(NH_3)_6^{3+}$ fails to correctly substitute for Mg^{2+} as its inert NH_3 ligands cannot dissociate from the metal center, which is in contrast to the aqua ligands of a Mg^{2+} ion. Indeed, such inner-sphere binding to nucleotides occurs quite commonly at the oxygen and nitrogen donor atoms of guanines and uracils, as well as at phosphate oxygens.[18] Nevertheless, to take part in the catalytic process, a metal ion does not need to be coordinated directly to the acting atoms, but can exert its influence also from a certain distance.[13] Therefore, to clarify the structural and metal-ion binding properties of the branch site, we have solved and investigated the solution structure of this region in the absence and presence of Mg^{2+}. Notably, the branch adenosine is under all conditions the only unpaired nucleotide at the branch site and is stacked between the two neighboring GU wobble pairs. Still, the branch 2'-OH protrudes out into the solvent. Furthermore, titration studies with Mg^{2+} by NMR revealed a metal ion binding site in the major groove of the branch site, placing this ion into close proximity of the catalytic center. This Mg^{2+} ion can thus exert a structural role as well as an electrostatic stabilization of the first transition state of splicing.

Results

NMR spectra of a minimal branch domain 6.

Wild type D6 consists of a hairpin structure with two helical stems flanking the branch adenosine. In some group II introns, like ai5γ from the yeast mitochondrial *cox1* gene, an internal loop structure is located within stem 2. Initial NMR spectra analyses of the full length D6 from ai5γ show that the six-nucleotide internal loop does not adopt a rigid structure under any conditions investigated. Thus, we studied a truncated construct (D6-27) from the wild-type (wt) sequence of D6 of the yeast group II intron ai5γ (Figure 1A and B). As the internal loop is neither phylogenetically conserved, nor contains important branch point determinants,[9] we removed nucleotides A859-U864 and G871-A876. D6-27 still encompasses the branch adenosine together with a minimum of three neighboring base pairs on either side, and thus metal ion binding at the branch site will not be affected by this mutation. To check the compatibility of our D6-27 sequence with group II intron reactivity, we performed trans-branching assays as described before.[10] Incorporation of our shortened D6 sequence into the standard two-domain construct D56 leads to an only slightly reduced activity as compared to the wt D56 sequence (Figure 2). Under the conditions applied (see Material and Methods), k_{obs}

values of 19.1 ± 0.1 min^{-1} (wtD56) and 13.9 ± 0.1 min^{-1} (D56-27) were obtained, and about 20% branched product is formed in both cases (it should be noted that reverse-branching is taking place simultaneously). The observed activity might seem surprising at first sight, as the removal of the internal loop in stem 2 should prevent tight docking of the tetraloop into its receptor in domain 2 (η-η' interaction). However, the only slightly reduced activity is well in line with recent studies[10] showing that the main determinant for proper branching is its covalent linkage to D5.

In accord with the observation that the shortened D6-27 is still active *in vitro*, the NOESY spectra of both the wt and the D6-27 constructs show identical peak patterns around the branch region (Supporting Information Figure S1) and reveal that only one conformation is present in solution. Two starting points for the sequential walk at the 5'-end were found. In accord with previous findings at nucleotides,[19] the G1H1' resonance at 5.923 ppm is attributed to the 5'-end with a triphosphate and the one upfield at 5.853 ppm with a monophosphate attached (a mixture of 5'-GMP and 5'-GTP was used[20] for transcription). These two starting points fall together at nucleotide A3. The 1:2 ratio of the volumes of the corresponding NOE resonances did not change during the course of the measurements, indicating that no hydrolysis of the triphosphate chain took place.

The sequential walk continues throughout the hairpin. ^{1}H NMR spectra in H_2O reveal imino protons of nine Watson-Crick and one GU wobble (G8-U19) base pairs, as well as the N1H proton of the sheared GA bp in the tetraloop. All imino resonances could be unambiguously assigned by the aid of [^{1}H,^{1}H]-NOESY, [^{15}N,^{1}H]-HSQC, and a 2D J_{NN} HNN-COSY in 90% H_2O / 10 % D_2O (see also Experimental Section). Regarding the second GU wobble 3' of the branch adenosine, no resonance for G7H1 and only a very broad signal corresponding to U21H3 is detected. This indicates that the wobble pair below the branch-point is nor properly formed and therefore imino-proton exchange with the solvent is not retarded. However, NOEs of the base protons of G7 and U21 to nucleobases above and below indicate stacking interactions in both strands.

The NOE peak pattern of the branch A20 is of special interest: The aromatic H8 shows intranucleotide NOE resonances to all sugar protons as expected for a usual anti conformation of the base. A NOE peak of A20H2 to the G8H1' on the opposite strand clearly places the branch adenosine within the helix (Figure 3). However, this H2 resonance at 7.62 ppm is more downfield shifted than the H2 located in an AU base pair but still more upfield than the tetraloop AH2s. The same holds for all proton-chemical shifts of A20. Such a chemical shift pattern indicates clearly that A20 is neither fully buried within the helix nor flipped out.

The structure of D6-27.

The structure determination of D6-27 is based on 589 conformationally restrictive NOE distance restraints (Table 1) (for details see Materials and Methods). The RNA adopts a stable hairpin with two well-defined helical regions flanking the branch A20 (Figure 1C). The overall r.m.s.d. of all heavy atoms from the 20 lowest energy structures is 1.18 ± 0.37 Å (Supporting Information Figure S2). Despite such a small r.m.s.d. a small deviation in the kink between the two helices is observed with the branch region being the hinge (Supporting Information Figure S2B and S2C, as well as r.m.s.d. values in Table 1).

The positioning of the branch A20 is of special interest. In solution, only A20 is unpaired but embedded within the helix between the two flanking GU wobble pairs (Figure 1C). The G8-U19 wobble right upstream of A20 is very well defined and stacks onto helix 2. In contrast, the G7-U21 wobble downstream of the branch site is staggered, but still well embedded within the helix (Figure 1C and Supporting Information Figure 2). G7 is pushed down towards G6 and out of the GU plane by the intruding A20, which itself stacks onto U21. As a consequence, both imino protons of G7 and U21 are no longer involved in stable base pairing, thus explaining the absence of sharp NMR signals for both. A20 itself is slightly edged out of the helix with its minor groove side including the branch 2'-OH increasingly solvent-exposed. This leads to a slight kink in the helix and a well accessible minor groove for possible tertiary contacts.

Localization of Metal Ion Binding Sites in D6-27 by Mg^{2+} Titration Studies.

Divalent metal ions are crucial for folding and catalysis of group II introns.[8] Indeed, several metal ions have been identified within the catalytic core.[5,6,15-17] Metal ion binding in the branch region of D6 has first been identified by hydrolytic cleavage experiments.[16] In addition, a $Co(NH_3)_6^{3+}$ molecule coordinated to O4 of U19 was found in the crystal structure of a D56 construct that shows a two-nucleotide branch site.[5] To obtain better information on the atomic level on the Mg^{2+} binding at the branch A, we now used NMR titration studies to determine the effect of Mg^{2+} on the structure of the branch site and other regions in D6. Changes in chemical shifts of imino protons are commonly recorded for this purpose. However, such data is often difficult to interpret,[6] as imino protons are located far away from the metal ion coordination site and their chemical shift is additionally dependent on the local structure and the exchange rate with the solvent. Even more important, adenine and cytosine moieties cannot be observed and metal ion binding to bulge regions can often not be followed, as these imino protons become broadened beyond detection.[6]

By recording [^{1}H,^{1}H]-NOESY spectra in D_2O, we excluded the effect of proton exchange with the solvent and were able to monitor effects of Mg^{2+} to the RNA at both the sugar and the

nucleobase residues. The observed H8, H2, H6, H5 and H1' protons are located right next to potential binding sites, e.g., N7 of purines, carbonyl oxygen atoms of both purines and pyrimidines, or 2'-OH at the sugar moieties. Titration of $MgCl_2$ to a solution of D6-27 in D_2O leads to increasing changes in chemical shifts of specific resonances throughout the hairpin. These changes in chemical shift, $\Delta\delta$, reflect very well the coordination of Mg^{2+} nearby and $\delta\Delta$ values both in upfield and downfield direction were extracted for all aromatic as well as H1' protons throughout D6-27 (Figure 4). It should be noted at this point that chemical shifts changes can be induced either by direct metal ion binding or by the structural changes that the coordination induces nearby, i.e. increased or reduced stacking interactions. A second effect observed during these titration studies is the substantial line broadening of some peaks. Line broadening upon addition of Mg^{2+} is well known and is allocated to an intermediate exchange of the Mg^{2+}(aq) ion at its binding site on the NMR time scale.[21,22] The line broadening can thus be used to detect specific Mg^{2+} sites, as it should only be observed at sites, where Mg^{2+} binds in very close proximity, e.g. H8 of a purine moiety is broadened upon Mg^{2+} binding to N7. By evaluating both of the above information a quite accurate picture of metal ion binding was obtained.

Most significantly, the chemical shifts of residues located around the branch point, i.e. the branch adenosine itself as well as those of the flanking GU wobble pairs, are strongest affected (Figure 4). In fact, A20H2 shows the largest overall chemical shift change of >0.25 ppm. The general picture of $\Delta\delta$ values shows that the resonances of the G8-U19 pair are stronger affected than those of the G7-U21 wobble, suggesting a Mg^{2+} coordination more on the side of the G8-U19 pair. Regarding the line broadening upon Mg^{2+} addition, it is interesting to note that the intraresidue crosspeak A20H1'-H8 is not affected, indicating that the metal ion at the branch site does not directly coordinate to the adenosine moiety. However, moderate line broadening is observed at signals belonging to the neighboring GU pairs. Indeed, these wobble pairs flanking the branch adenosine form a perfect Mg^{2+} binding site: The carbonyl groups of the two GU wobble pairs, the N7 positions of the purine nucleobases as well as the oxygen atoms of the phosphate groups are perfectly located (Supporting Information Figure S3). The calculated electrostatic surface potential map further supports this interpretation showing a highly negatively charged area in the major groove (Figure 1D and Supporting Information Figure 2). The major groove of GU wobble pairs is a well known metal ion binding site[23-25] and thus the here presented data means that an intercalated adenosine does not disrupt this coordination ability.

The strongest line broadening effects were observed at the 5'-end for G1, G1a, G2 and even A3. In addition, also the aromatic protons as well as H1' of C27 at the 3'-helix end

experience changes in chemical shifts. This observation corresponds well to the presence of the 5'-terminal phosphate group(s), being the strongest binding site due to their multiple negative charge. The interresidual crosspeak between A3 H1' and G4 H8 shows no effect but G4 H1'-H8 broadens above average at around 8 mM Mg^{2+}, indicating a possible further Mg^{2+} binding site at the tandem GC base pair in helix 1.

A third set of strongly affected chemical shifts is found at nucleotides in and right below the tetraloop (Figure 4). Along this line also resonances belonging to A15, A16 and C17 are broadened upon addition of Mg^{2+}. Metal ion binding to GNRA tetraloops is known,[6,21,26,27] however, the nucleotides around the tetraloop, of which the resonances are affected one and/or the other way, span a range of 13-14 Å being to large to be covered by one specifically bound metal ion. As proposed by fluorescence studies[28] of a tetraloop structure, it is well feasible that two Mg^{2+} ions bind in close proximity at this site, even though one could also picture one Mg^{2+} ion "rolling" over the whole tetraloop region. Indeed, it has been shown before that nucleic acids can accommodate two metal ions in surprisingly close neighborhood to each other,[29,30] and that their binding affinity is hardly affected.[30]

Taken together, the accumulated data from out Mg^{2+} titration studies reveal the following metal ion binding regions in the shortened branch hairpin D6-27: The helix end, the tandem GC pair in helix 1, the branch-site and the tetraloop. The resonances at the 5'-end as well as C27 are affected most at low Mg^{2+} concentrations. As one would expect, this indicates that the phosphate groups show the highest affinity towards metal ions within an *in vitro* transcribed RNA. The extent of chemical shift changes vary substantially for the other three to four binding sites within D6-27 (Figure 4), suggesting also large differences in binding affinities. However, the amount of line broadening runs almost parallel at the observed resonances. The latter observation is a strong indication that actually these binding sites within the branch domain are occupied simultaneously with similar affinities (a detailed evaluation of the affinity constants within D6-27 will be published elsewhere).

Does the Branch Site Changes its Structure upon Mg^{2+} Binding?

It is important to understand how the binding of divalent metal ions affects the geometry of local RNA structures. A recent study reported the branch adenosine to change its positioning between the two adjacent GU wobble pairs upon addition of Mg^{2+}.[31] We confirmed these findings by titrating a D6-27 construct, where the branch-adenosine was replaced by a 2-aminopurine with Mg^{2+} and monitoring the fluorescence emission at 371 nm. In agreement with experiments performed by Schlatterer et al.,[31] we detected a quenching of the 2-aminopurine fluorescence, indicative of increased stacking of the branch-A within the D6-27 helix. The plot

of the emission maxima versus [Mg^{2+}] could be fitted to an exponential decay, flattening out around 50 mM Mg^{2+} (Figure 5). Interestingly, this number is close to the minimal Mg^{2+} concentration that is needed for folding and activity of ai5γ in vitro.[14]

The fluorescence studies with 2-aminopurine only yield a qualitative picture on the positioning of the branch-adenosine as the amount of fluorescence quenching (or enhancement) for the fully stacked (or fully flipped out) nucleobase is not directly accessible. Consequently we observed with great care the NOESY pattern of the branch region, i.e. crosspeaks involving U19, A20, U21 and the opposite strand at G7 and G8, upon increasing amounts of Mg^{2+}. All signals of the sequential walk as well as the intranucleobase aromatic-to-aromatic crosspeaks are clearly visible to concentrations larger than 6 mM $MgCl_2$. At higher concentrations some of the signals become very broad (see also above). Also around the branch site some line broadening is observed, but the sequential walk remains visible. This is a clear indication that the structure around the branch adenosine does not change dramatically upon Mg^{2+} binding. A further proof for this assessment is the fact that the interstrand NOE crosspeak between A20 H2 and G8 H1' is still visible at 12 mM Mg^{2+}. This crosspeak can only show up when the branch-A remains stacked within the helix.

Discussion

This study is the first report of a NMR solution structure of the D6 branch-site from a group II intron ribozyme, including a detailed investigation of its metal ion binding properties. The construct used in this study lacks the internal loop above the branch site, but trans-branching assays show an almost wild-type like activity. These results corroborate with phylogenetic data[9,10] that indeed no crucial branch point determinants are present in the omitted nucleotides and that the length of the helix above the branch adenosine is not important for docking to the other domains and branching

The branch site geometry has been a matter of debate and two different conformations of the branch site in group II introns have been suggested in the past: A two-nucleotide bulge with a shifted base pairing pattern 5' of branch A was found in the crystal structure of a coaxially stacked D56 construct.[5] In contrast, phylogenetic and mutational studies favor a single non-paired branch A with a conserved GU wobble upstream thereof.[10]

The here described solution structure of D6-27 with a single unpaired branch-adenosine between two A-form helices concurs exactly with the prediction from phylogeny and differs considerably from the crystal structure of a D56 construct. In the crystallized construct domain 6 is not closed by a GUAA tetraloop but has an open helix end, one of whose strands folds back and stacks onto the branch A, thus possibly inducing the shift in base pairing. N3 alkylation with

CMCT (1-cyclohexyl-3-(2-morpholinoethyl) carbodiimide metho-*p*-toluene sulfonate)[5] revealed a strong modification of U881 in both wt D56 and the crystallized construct, indicative of an exposed Watson-Crick face of these uridine moieties. While such an increased reactivity of U881 was taken as an indication for a two-nucleotide bulge, it can also be explained by our here presented data: The staggering of the G7-U21 wobble pair leads to an increased solvent exposure of the Watson-Crick face of both nucleobases. This makes U21 (i.e., U881 in the wt sequence) accessible for CMCT modification even in the presence of a single nucleotide bulge. The solvent accessibility is corroborated by severe line broadening of the imino resonances for both nucleobases as observed by NMR. Only the phylogenetically conserved[10,32] wobble pair 5' of A20 forms a rigid base pair in solution, whereas the G7-U21 is poorer defined.

How does our structure of D6 compare to the situation in the spliceosome? In the light of the eminent mechanistic similarities and the proposed evolutionary relationship, it is tempting to assume structural analogies between group II introns and the spliceosome. However, it is important to note that many differences exist in terms of branch-site recognition and function.[10,33] For example, in yeast, where the two systems are most closely related, the spliceosomal branch-A is not flanked by GU-wobbles, a feature that is highly conserved in group IIB introns.[10] Instead, a conserved spliceosomal seven nucleotide sequence[34] together with a pseudouridine opposite to the branch adenosine are likely to be responsible for the single bulged-out branch A,[35] which must be unpaired for successful splicing. In the group II intron ai5γ on the other hand, a base paired branch A does not completely abolish branching.[9] In all eukaryotic spliceosome systems investigated to date, a pseudouridine (Ψ) residue opposite of the branch-point adenosine has been identified.[36,37] NMR structural analyses have shown that this Ψ is responsible for an extrahelical positioning of the branch adenosine in the isolated branch helix.[35,38] Although no Ψ has been identified in group II introns to date, the relationship with the spliceosome makes a bulged-out adenosine in context of the whole group II intron also tempting to propose. However, in the light of the many differences between the two systems and the here presented solution structure of an active D6 construct, the occurrence of a helically stacked branch adenosine should be considered more closely. In our structure, a slight kink in the helix around the branch point is introduced by the intruding A together with the optimized stacking of U21 to A20 at the cost of U21-G7 base pairing. This opens the minor groove to make the 2'-OH of the branch-point increasingly accessible for tertiary contacts. These findings are well in line with the observation that A20→X mutations with nucleobases of lesser stacking ability[19,39] lead to reduced branching.[33]

Metal ions are key players in group II intron ribozymes, not only stabilizing the complicated tertiary structure, but also being directly implicated in catalysis.[8,14,15] Therefore we

have put a strong emphasis on the detailed investigation of metal ion binding sites within our structure. It is evident that any larger RNA oligonucleotide will exhibit several metal ion binding sites due to the manifold negative charges present. At this stage we propose up to four or five specific Mg^{2+} binding sites in D6-27, namely at the 5'-end of the hairpin, the tandem GC base pair in helix 1, the branch-region and one or two metal ions binding to the tetraloop. Mg^{2+} titration and 2-aminopurine fluorescence studies indicate that the local structure around the branch-point does not change upon metal ion binding. If at all, Mg^{2+} rather seems to lead to an increased stacking of the branch-A within the helix of D6-27. Fluorescence studies with the wt D6[31] indicate that the internal loop in helix 2 has some influence on the positioning of the branch adenosine. However, this influence is obviously of no big concern for the binding of D6 to the catalytic core as well as to the activity of the ribozyme itself as our activity essays with D6-26 show. To us it seems more important that (i) a Mg^{2+} ion is bound to the major groove at the branch site and that (ii) even a minimal domain 6 binds three-to-four additional Mg^{2+}. This relatively high number of Mg^{2+} ions bound specifically and with similar affinities to such a short hairpin ensures that the branch domain can be dragged more easily into and bound to the negatively charged and closely-packed catalytic core. Hence, D6 represents a second example besides the adjacent domain 5[6] of a small hairpin serving a metal ion binding platform before being bound to the catalytic center.

The here identified Mg^{2+} in the major groove of the branch site is certainly of great interest, being that close to the catalytic site. Based on the here presented data we suggest the following picture: Metal ion binding is restricted to the neighboring GU pairs, and does not include the adenine N7. This would mean that the intercalated adenine base does not disrupt the potential of GU wobbles to bind Mg^{2+} ions. The strong downfield shifts of A20s H8 and H2 are therefore due to a structural change at the branch site: M^{2+} binding to the carbonyl oxygens pulls the flanking wobble pairs closer together leading to a stronger kink within D6 and a subsequent stronger exposure of A20s 2'-OH. Nevertheless, the NOE pattern of the interstrand NOE of A20 H2 to G8 H1' shows that also at higher Mg^{2+} concentration up to a 15 fold excess of Mg^{2+} over RNA, the branch A20 remains stacked within the helix. This is in agreement with fluorescence studies performed by us and others[31] which show fluorescence quenching in a D6 construct without its internal loop, where an aminopurine substitutes for the branch-A, upon addition of Mg^{2+}. Thus, in the light of the present results, that the branch adenosine remains stacked to a large part within the helix, one may question if group II introns are structurally really that closely related to the eukaryotic spliceosome as superficial similarities in the catalytic mechanisms imply.

One should note that despite not being directly coordinated at the A20, the observed Mg^{2+} will still have an important impact on catalysis. When coordinated to the carbonyl oxygens of the GU wobble pairs, the bound Mg^{2+} is located only about 10 Å from A20s O2'. The metal ion is thus close enough to contribute in an electrostatic manner to the stabilization of the build-up negative charge in the transition state during splicing. Such electrostatic effects from a distance must not be underestimated as detailed experiments with the protein subtilisin show,[40,41] and should thus be seriously considered also in ribozyme chemistry.[13]

Experimental Section

Materials: DNA oligonucleotides were purchased from Microsynth, Balgach (Switzerland), and the nucleotide 5'-triphosphates came from GE Healthcare (formerly Amersham Biosciences Europe GmbH), Otelfingen (Switzerland)), except for UTP, which was obtained from Sigma-Aldrich-Fluka, Buchs (Switzerland). T7 polymerase used for *in vitro* transcription was homemade.[20,42] The electroelution apparatus *Biotrap* was from Schleicher & Schuell, Dassel (Germany). For desalting, Centricon Centrifugal Filter Devices (3000 MWCO) from Amicon were used. ^{13}C,^{15}N-labeled D6-27 was transcribed from isotopically labeled NTPs from Silantes GmbH, München (Germany). D6-27 with a 2-aminopurine at the branch-site, D6-27(2AP), was ordered in a 0.2 μM synthesis scale from Dharmacon Inc., Chicago, IL (USA). $MgCl_2$ for the metal ion titration was obtained as 1M ultrapure solution in H_2O from Fluka-Sigma-Aldrich, Buchs (Switzerland). The exact concentration of the $MgCl_2$ and $MnCl_2$ stock solution in 99.999% D_2O (Sigma-Aldrich) was determined by potentiometric pH titration employing EDTA. All chemicals used were at least puriss p.a. and purchased from either Fluka-Sigma-Aldrich, Buchs (Switzerland) or Brunschwig Chemie, Amsterdam (The Netherlands).

Activity assays: wtD56 and D56-27 were transcribed by T7 polymerase from linearized plasmids pT7-56[43] and pME1c. pME1c was obtained by cloning the D56-27 construct including a T7 promotor at the 5'-end by assembly-PCR and insertion into a standard cloning vector at HindIII and EcoRV restriction sites. wtD56 and D56-27 were both labeled with ^{32}P at the 5'-end. Trans-branching assays were conducted as previously described,[10] except that pH 7.2 (instead of pH 7.5) and NH_4Cl (instead of $(NH_4)_2SO_4$) was used. Concentrations used were 5 nM (D56) and 2 μM (exD123). The k_{obs} values were calculated based on a pseudo-first order reaction kinetic.[44]

NMR sample preparation: D6-27 (5'-GGAGCGGGGGUGUAAACCUAUCGCUCC) and D6 (5'-GGAGGGGGAAAACUUGUAAAGGUCUACCUAUCUCC), i.e. the wt sequence with the 5'-CC replaced by GGA and its complement at the 3'-end to increase transcription yields) were synthesized by *in vitro* transcription with T7 polymerase from a double stranded DNA template.[20] All RNA was purified by denaturing 18% PAGE, UV-shadowed, excised from the gel and recovered by electroelution. After desalting and lyophilization, the sample was dissolved in 220 µL D_2O (100 mM KCl, 10 µM EDTA, pD 6.7). To measure the pD value, 0.4 log units were added to the pH meter reading.[45,46] The RNA concentration was determined with a Varian Cary 500 Scan UV-VIS-NIR spectrophotometer, using an extinction coefficient at 260 nm (ε_{260}) of 296.3 $mM^{-1}cm^{-1}$ for D6-27 and 403 $mM^{-1}cm^{-1}$ for D6. The concentrations of the RNA samples varied between 0.2 and 1.1 mM. All samples were lyophilized and resuspended in either 90% H_2O/10% D_2O or 99.999% D_2O prior to acquisition of NMR spectra.

NMR spectroscopy: NMR spectra were recorded on a Bruker DRX 500 MHz spectrometer using a 5 mm BBI probehead or on a Bruker AV700 MHz spectrometer equipped with a CP-TXI z-axis pulsed-field gradient cryoprobe. Non-exchangeable proton resonances were assigned from 2D [^{1}H,^{1}H]-NOESY spectra acquired at 303 K (50, 120 and 250 ms mixing times) and 308 K (250 ms mixing time), [^{1}H,^{1}H]-TOCSYs (45 ms mixing time), [^{13}C,^{1}H]-HSQCs that were recorded separately for the aromatic and the aliphatic range of the ^{13}C resonances as well as 3D [^{13}C,^{1}H,^{1}H]-HCCH COSY and 3D [^{13}C,^{1}H,^{1}H]-HCCH TOCSY experiments. Exchangeable proton resonances were assigned from 2D [^{1}H,^{1}H]-NOESY spectra acquired at 275 K and 283 K with mixing times of 150 ms and watergate H_2O suppression, and by the aid of a [^{15}N,^{1}H]-HSQC. The base pairing scheme was established by a 2D J_{NN} HNN-COSY,[47] correlating the imino nitrogens of uracil (N3) and guanine (N1) across the H-bond to the N1 of adenine or the N3 of cytosine on the other side of the double helix. Additional [^{1}H,^{1}H]-NOESY spectra were recorded at pH 6.1 and 5.0 to check for possible perturbed pK_a values and structural changes. No structural changes were observed at pH 6.1. At pH 5.0 NOE resonances became much broader, which is expected as the buffer region of protonated adenosine N1 and cytosine N3 positions is reached. NMR spectra were processed with XWINNMR and TOPSPIN 3.1 (Bruker) and analyzed using Sparky (http://www.cgl.ucsf.edu/home/sparky/). NOE peak volumes were integrated with the Gaussian peak fitting function in Sparky.

Structure calculation: NOE distances were estimated from the integrated peak volumes obtained from the [^{1}H,^{1}H]-NOESY spectrum that was acquired at 303 K with a mixing time of 250 ms. Distances were calibrated using the CALIBA macro in DYANA.[48] The NOEs were

grouped into four categories, corresponding to strong (1.8 – 3 Å), medium (1.8 – 4.5 Å), weak (3.0 – 6.0 Å), and very weak (4.0 –7.0 Å). NOEs obtained from [^{1}H,^{1}H]-NOESY peaks in 90% H_2O/10% D_2O were qualitatively assigned as strong, medium, weak or very weak. Based on 1D ^{31}P NMR spectra, the torsion angles α and ζ (except for A15, which was left unconstrained, as well as A14 and C27, where only α was constrained) were set to exclude the trans-range.[49] Sugar pucker restraints were included based on TOCSY experiments with a 45 ms mixing time.[6] G1 showed strong H1'-H2' and H1'-H3' crosspeaks and was restrained to S-type (δ = 145 ± 20º). G12, U13, A14, A15, U19, A20 and C27 were left unconstrained. All other nucleotides showed no H1'-H2' crosspeak and were therefore constrained to N-type (δ = 85 ± 20º). The other backbone torsion angles (β, γ, ε) were set to standard A-form values only in the helical regions of the structure known to be A-form (G2-U11, A16-C18, U21-C26). Based on the H1'-aromatic NOEs from the 50 ms [^{1}H,^{1}H]-NOESY, the torsion angle χ was restrained to –160 ± 20º (anti) for all residues except A20, which was left unconstrained. Additional H-bond restraints were added for base pairs whose existence was proven by ^{1}H,^{1}H crosspeaks across the helix in the imino region and by HN-crosscorrelations from the 2D J_{NN} HNN-COSY.[47] The structure calculations were performed using XPLOR-NIH.[50] The twenty structures with the lowest XPLOR energies out of 200 calculated were analyzed using MOLMOL.[51] The electrostatic surface potentials of D6-27 was calculated using QNIFFT [52] and visualized with PYMOL (W. L. DeLano, 2002, http://www.pymol.org).

Mg^{2+} titration studies: The concentration of D6-27 RNA in the titration experiments was 0.85 mM. Mg^{2+} binding to D6-27 was monitored by observing the linebroadening and changes in chemical shifts of the aromatic and sugar protons in [^{1}H,^{1}H]-NOESY spectra acquired in the presence of 0, 1, 2, 3, 4, 5, 6, 7, 8, 10, and 12 mM $MgCl_2$ (99.999% D_2O, I = 0.1 M (KCl), 10 μM EDTA, pD = 6.7). In addition, the chemical shift changes of the imino-protons upon addition of Mg^{2+} were monitored by [^{1}H]-NMR spectra in presence of 0, 1, 2, 4, 6, 8, 10, 13, 16, 20, 25 and 30 mM $MgCl_2$.

2-aminopurine fluorescence: D6-27(2AP) was purified by reversed phase chromatography, using a Beckmann Coulter Ultrasphere column on a Merck Hitachi Elite La Chrom HPLC system. The binding buffer contained 0.1 M triethylammonium acetate at pH 7. An optimized gradient elution run was performed using 100 % Acetonitrile (Biosolve). The RNA was eluted after a retention time of 30 min at a flow rate of 1 ml/min. A final stock solution of D6-27(2AP) of 81.7 μM in 40 mM MOPS, 10 μM EDTA, pH 7.2 was prepared. The concentration was determined via UV detection at 260 nm with an extinction coefficient of 246.6 $mM^{-1}cm^{-1}$. To

avoid dilution effects on addition of Mg^{2+} during the fluorescence measurements, the metal ion solutions were prepared as to contain the same concentration of RNA as the starting solution. 25 mM DTT was added to avoid oxidation. The starting solution (A) contained 1 μM D6-27(2AP), 25 mM DTT and 10 mM MOPS, pH 7.2. Two different stocks of Mg^{2+} containing solutions were prepared (B100 and B500), also containing 1 μM D6-27(2AP), 25 mM DTT and 10 mM MOPS, pH 7.2 and additionally either 100 mM (B100) or 500 mM (B500) $MgCl_2$ from a 1M potentiometrically titrated stock solution. All solutions were heated up to 95 °C for 1 min to destroy any alternative secondary folds and slowly left to cool. All samples were degassed in an Eppendorf Concentrator 5301 and the lost volume was refilled with H_2O. All experiments were carried out with a scan speed of 100 nm/min, an excitation slid of 5.0 nm and an emission slid of 10 or 15 nm. The excitation wavelength was set to 305 nm. Emission scans were performed from 330 – 420 nm. Two measurement series were performed, with 0, 0.5, 1, 3, 5, 7, 9, 13, 17, 21, 25, 30, 35, 40, 45, 50, 70, 90, 110, 130, 150 and 200 mM Mg^{2+} as well as 0, 0.1, 0.3, 0.5, 0.7, 1, 3, 7, 11, 15, 20, 25, 30, 40, 50, 70, 90, 100, 110, 130, 150 and 200 mM Mg^{2+}.

Acknowledgements

We thank Anna Marie Pyle, Yale University, for encouragement and a generous gift of labeled NTPs, and Dipali Sashital and Samuel E. Butcher, University of Wisconsin, as well as Nadja Bross-Walch and Simon Jurt from the NMR facility of the University of Zürich for helpful suggestions regarding the NMR measurements, Olga Fedorova, Yale University, for helpful advice concerning the trans-branching assay, and Bernd Knobloch for the preparation of the $MgCl_2$ stock solution in D_2O. Financially support by the Swiss National Science Foundation (SNF-Förderungsprofessur to R.K.O.S., PP002-68733/1) is gratefully acknowledged.

Supporting information

Supporting Information includes a comparison of [^{1}H,^{1}H]-NOESY spectra of wtD6 and D6-27, an overlay of the twenty lowest energy structures, a picture of the calculated surface potentials of the minor groove side of the branch region as well as the arrangement of potential Mg^{2+} coordinating atoms in the major groove at the branch site. This material is available free of charge from the Wiley website.

References

[1] K. Lehmann, U. Schmidt, *Critical Rev. Biochem. Mol. Biol.* **2003**, *38*, 249.

[2] J. D. Boeke, *Genome Res.* **2003**, *13*, 1975.

[3] S. E. Butcher, D. A. Brow, *Biochem. Soc. Trans.* **2005**, *33*, 447.

[4] T. W. Nilsen, *Encyclop. Biol. Chem.* **2004**, *4*, 88.

[5] L. Zhang, J. A. Doudna, *Science* **2002**, *295*, 2084.

[6] R. K. O. Sigel, D. G. Sashital, D. L. Abramovitz, A. G. Palmer III, S. E. Butcher, A. M. Pyle, *Nat. Struct. Mol. Biol.* **2004**, *11*, 187.

[7] A. de Lencastre, S. Hamill, A. M. Pyle, *Nature Struct. Mol. Biol.* **2005**, *12*, 626.

[8] R. K. O. Sigel, *Eur. J. Inorg. Chem.* **2005**, *12*, 2281.

[9] V. T. Chu, Q. Liu, M. Podar, P. S. Perlman, A. M. Pyle, *RNA* **1998**, *4*, 1186.

[10] V. T. Chu, C. Adamidi, Q. Liu, P. S. Perlman, A. M. Pyle, *EMBO J.* **2001**, *20*, 6866.

[11] R. K. O. Sigel, A. M. Pyle, *Met. Ions Biol. Syst.* **2003**, *40*, 477.

[12] R. K. O. Sigel, H. Sigel, *Met. Ions Life Sci.* **2007**, *2*, 109.

[13] R. K. O. Sigel, A. M. Pyle, *Chem. Rev.*, *in press*.

[14] J. F. Swisher, L. J. Su, M. Brenowitz, V. E. Anderson, A. M. Pyle, *J. Mol. Biol.* **2002**, *315*, 297.

[15] P. M. Gordon, E. J. Sontheimer, J. A. Piccirilli, *Biochemistry* **2000**, *39*, 12939.

[16] R. K. O. Sigel, A. Vaidya, A. M. Pyle, *Nat. Struct. Biol.* **2000**, *7*, 1111.

[17] P. M. Gordon, J. A. Piccirilli, *Nat. Struct. Biol.* **2001**, *8*, 893.

[18] D. J. Klein, P. B. Moore, T. A. Steitz, *RNA* **2004**, *10*, 1366.

[19] K. H. Scheller, F. Hofstetter, P. R. Mitchell, B. Prijs, H. Sigel, *J. Am. Chem. Soc.* **1981**, *103*, 247.

[20] S. Gallo, M. Furler, R. K. O. Sigel, *CHIMIA* **2005**, *11*, 781.

[21] J. H. Davis, M. Tonelli, L. G. Scott, L. Jaeger, J. R. Williamson, S. E. Butcher, *J. Mol. Biol.* **2005**, *351*, 371.

[22] V. L. Pecoraro, J. D. Hermes, W. W. Cleland, *Biochemistry* **1984**, *23*, 5262.

[23] A. M. Pyle, *J. Biol. Inorg. Chem.* **2002**, *7*, 679.

[24] I. Tinoco, Jr., C. Bustamante, *J. Mol. Biol.* **1999**, *293*, 271.

[25] F. H.-T. Allain, G. Varani, *Nucleic Acids Res.* **1995**, *23*, 341.

[26] H. A. Heus, A. Pardi, *Science* **1991**, *253*, 191.

[27] S. Rüdisser, I. Tinoco, Jr., *J. Mol. Biol.* **2000**, *295*, 1211.

[28] M. Menger, F. Eckstein, D. Porschke, *Biochemistry* **2000**, *39*, 4500.

[29] C. C. Correll, B. Freeborn, P. B. Moore, J. A. Steitz, *Cell* **1997**, *91*, 705.

[30] B. Knobloch, R. K. O. Sigel, B. Lippert, H. Sigel, *Angew. Chem., Int. Ed.* **2004**, *43*, 3793.

[31] J. C. Schlatterer, S. H. Crayton, N. L. Greenbaum, *J. Am. Chem. Soc.* **2006**, *128*, 3866.

[32] F. Michel, K. Umesono, H. Ozeki, *Gene* **1989**, *82*, 5.

[33] Q. Liu, J. B. Green, A. Khodadadi, P. Haeberli, L. Beigelman, A. M. Pyle, *J. Mol. Biol.* **1997**, *267*, 163.

[34] R. Parker, P. G. Siliciano, C. Guthrie, *Cell* **1987**, *49*, 229.

[35] M. I. Newby, N. L. Greenbaum, *Nat. Struct. Biol.* **2002**, *9*, 958.

[36] J. Gu, J. R. Patton, S. Shimba, R. Reddy, *RNA* **1996**, *2*, 909.

[37] S. Massenet, Y. Motorin, D. L. J. Lafontaine, E. C. Hurt, H. Grosjean, C. Branlant, *Mol. Cell. Biol.* **1999**, *19*, 2142.

[38] M. I. Newby, N. L. Greenbaum, *RNA* **2001**, *7*, 833.

[39] P. R. Mitchell, H. Sigel, *Eur. J. Biochem.* **1978**, *88*, 149.

[40] A. J. Russell, P. G. Thomas, A. R. Fersht, *J. Mol. Biol.* **1987**, *193*, 803.

[41] S. E. Jackson, A. R. Fersht, *Biochemistry* **1993**, *32*, 13909.

[42] P. Davanloo, A. H. Rosenberg, J. J. Dunn, F. W. Studier, *Proc. Nat. Acad. Sci. U. S.* **1984**, *A81*, 2035.

[43] K. Chin, A. M. Pyle, *RNA* **1995**, *1*, 391.

[44] O. Fedorova, L. J. Su, A. M. Pyle, *Methods* **2002**, *28*, 323.

[45] R. Lumry, E. L. Smith, R. R. Glantz, *J. Am. Chem. Soc.* **1951**, *73*, 4330.

[46] P. K. Glasoe, F. A. Long, *J. Phys. Chem.* **1960**, *64*, 188.

[47] B. Luy, J. P. Marino, *J. Am. Chem. Soc.* **2000**, *122*, 8095.

[48] P. Güntert, C. Mumenthaler, K. Wüthrich, *J. Mol. Biol.* **1997**, *273*, 283.

[49] G. Varani, F. Aboulela, F. H. T. Allain, *Prog. Nucl. Mag. Res. Sp.* **1996**, *29*, 51.

[50] C. D. Schwieters, J. J. Kuszewski, N. Tjandra, G. M. Clore, *J. Magn. Res.* **2003**, *160*, 65.

[51] R. Koradi, M. Billeter, K. Wüthrich, *J. Mol. Graphics* **1996**, *14*, 29.

[52] K. Chin, K. A. Sharp, B. Honig, A. M. Pyle, *Nat. Struct. Biol.* **1999**, *6*, 1055.

Figure Captions

Figure 1. (A) Schematic representation of a group II intron with its six domains. D6 is colored in red and the branch A is indicated. (B) The wildtype D6 (top, together with the numbering scheme of the full group II intron) and the shortened D6-27 (bottom) constructs with the numbering scheme used in this study. The branch-A20 is shown in red and the two adjacent GU wobble pairs in gold. (C) NMR structure of D6-27. View of the lowest energy structure of D6-27. Helix 1 (nucleotides G1-G6, C22-C27) is colored in blue and helix 2 (nucleotides G9-C18) in green, the branch A20 in red (its 2'-OH is indicated by an arrow), and the two flanking GU wobble pairs in gold. (D) Calculated surface potential of D6-27. Red indicates negative, white neutral, and blue positive charges (red, –60; white –5; blue, 5 kTe^{-1}). D6-27 is turned counterclock-wise by 90°, thus offering a glance into the major groove behind the branch region, which is highly negatively charged (arrow). It can also be seen that the two phosphate-sugar backbones come very close together.

Figure 2. Activity tests of the shortened D6-27 construct. (A) Scheme of the trans-branching assay to test the activity of D6. The two-domain constructs wtD56 and D56-27 are each ^{32}P-labeled at the 5'-end (asterisk) and the 5'-exon is indicated as a grey line. The reaction conditions are the same as previously described,[10] except that NH_4Cl instead of $(NH_4)_2SO_4$, and pH 7.2 were used. (B) Secondary structures of wtD56 (left) and D56-27 (mutated) with a shortened D6 sequence according to the D6-27 sequence (right). Below, the reduction of the precursor band and the appearance of the product band of ^{32}P-labeled D56 constructs attached to D123 over time for the wtD56 (columns 1-8) and D56-27 (column 9-16) constructs are shown (5%/18% stacking gel). Time points are given in minutes. Clearly, the shortened D56-27 shows activity, which is only slightly reduced.

Figure 3. Evidence for the stacked branch adenosine. Part of the NOESY spectrum at 293 K showing the crosspeaks between A20 H2 and G8 H1' positioned across the helix. The sequential walk around the branch A as well as on the opposite strand is shown by solid black lines and connectivities with A20H2 are indicated by dotted lines. The U21 H5-H6 NOE peak is marked by a circle.

Figure 4. Chemical shift changes of D6-27 upon titration with 12 mM Mg^{2+}. The upper panel shows the difference in chemical shift between 0 and 12 mM Mg^{2+} for the aromatic H6 and H8 protons (light colors) as well as H2 and H5 (dark colors). In the lower panel the chemical shift changes of the H1' sugar protons are shown.

Figure 5. Fluorescence emission of 2-aminopurine in D6-27 upon excitation at 305 nm. The emission maximum at 371 nm plotted versus the Mg^{2+} concentration shows a reproducible fluorescence quenching, indicative of increased stacking of the branch-nucleobase between the two adjacent GU wobble pairs within the helix.

Table 1. NMR restraints and structural statistics for the D6-27 structure.[a]

NOE-derived distance restraints	589	
Intranucleotide	224	
Internucleotide ($\|i - j\| = 1$)	265	
Long-range ($\|i - n\| \geq 2$)	100	
Repulsive	0	
NOE restraints per residue	21.8	
Dihedral restraints	190	
Hydrogen bond restraints	59	
r.m.s.d. (for all heavy atoms to the best structure (Å)		
Overall		1.18 ± 0.37
Helix 1 (1-6, 22-27)		0.56 ± 0.19
Branch region (7, 8, 19-21)		0.43 ± 0.11
Helix 2, incl. GUAA (9-18)	0.57 ± 0.22	
NOE violations > 0.2 Å	0	
Dihedral violations > 5°	0	

[a] All statistics are given for the 20 lowest energy structures out of 200 calculated structures.

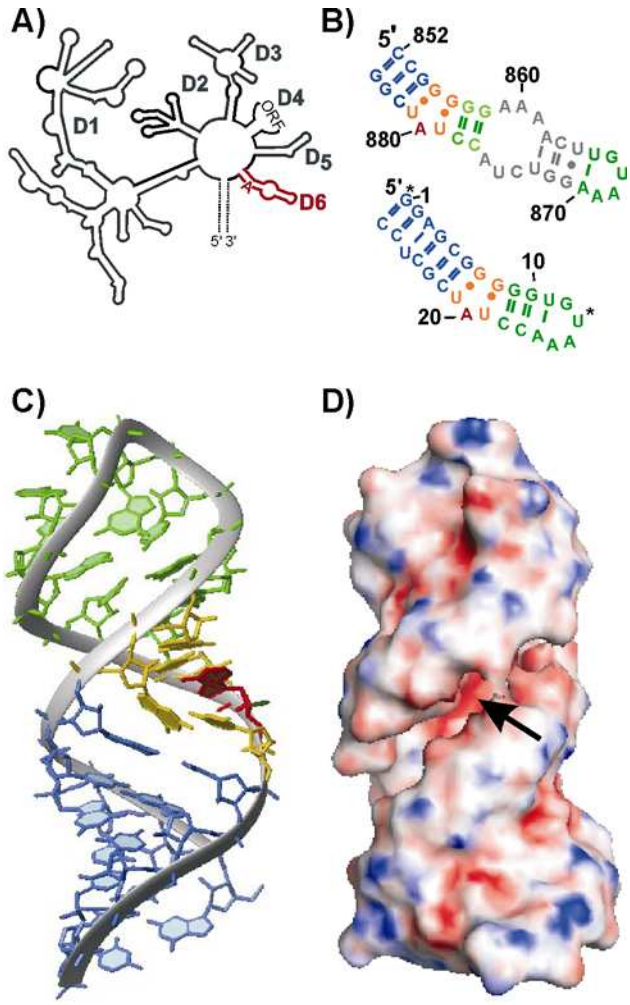

Figure 1

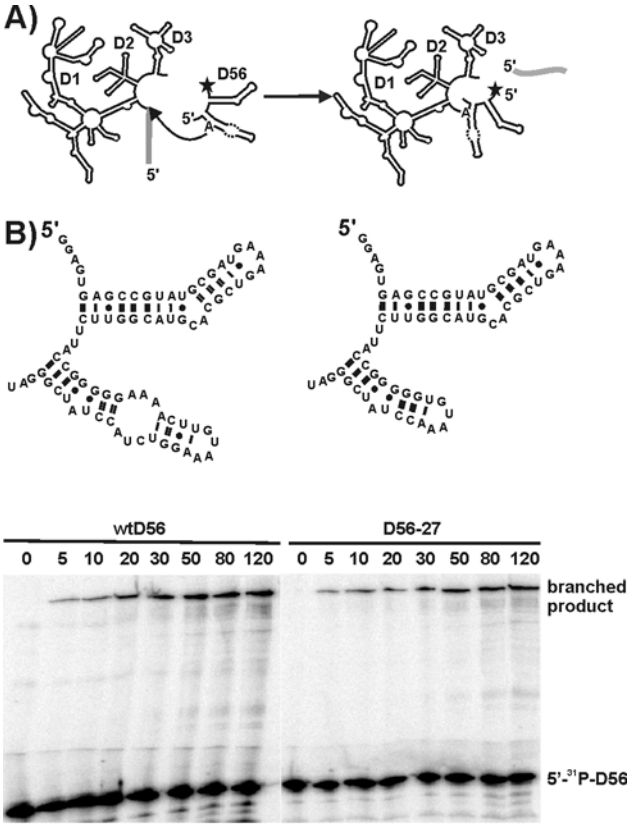
A)
D1
D2
D3
D56
5'
5'
A
B)
5'
wtD56
D56-27
0 5 10 20 30 50 80 120
0 5 10 20 30 50 80 120
branched product
5'-32P-D56

Figure 2

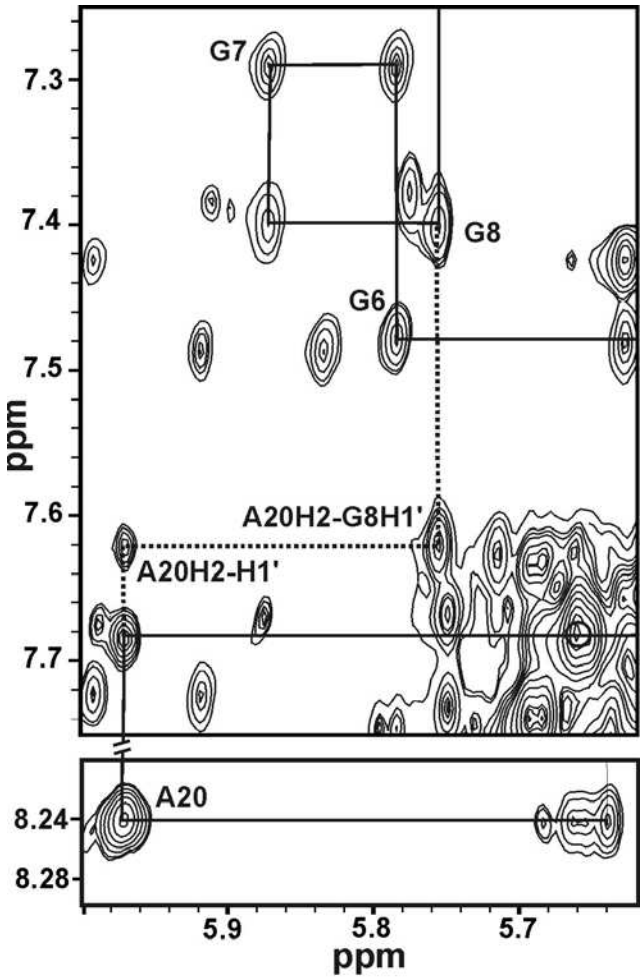
G7
G8
G6
A20H2-G8H1'
A20H2-H1'
A20
7.3
7.4
7.5
7.6
7.7
8.24
8.28
ppm
5.9
5.8
5.7
ppm

Figure 3

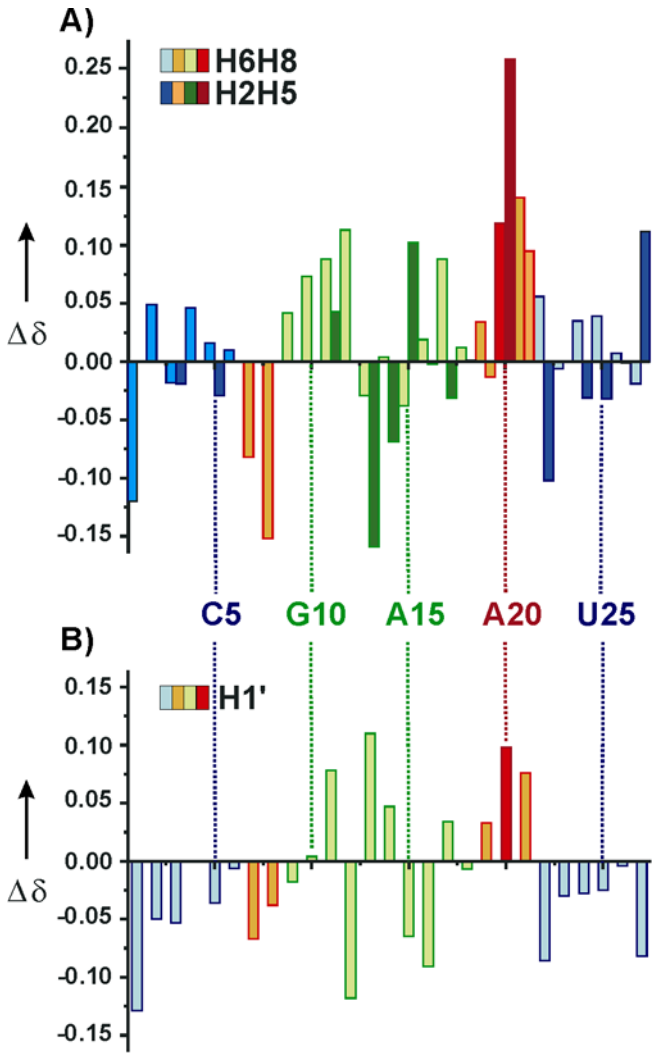
A)
H6H8
H2H5
0.25
0.20
0.15
0.10
0.05
0.00
-0.05
-0.10
-0.15
Δδ
C5
G10
A15
A20
U25
B)
H1'
0.15
0.10
0.05
0.00
-0.05
-0.10
-0.15
Δδ

Figure 4

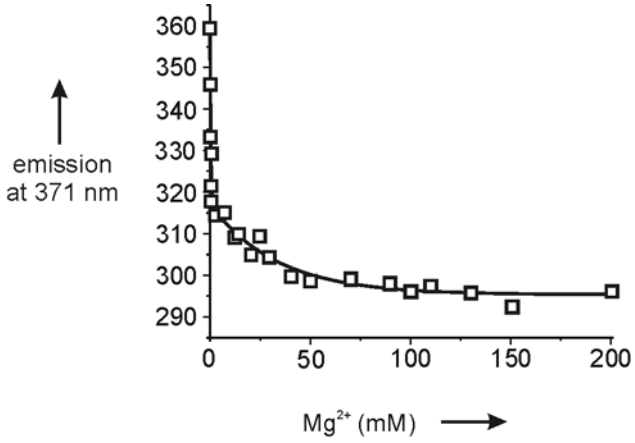
emission
at 371 nm
360
350
340
330
320
310
300
290
0
50
100
150
200
Mg2+ (mM)

Figure 5

for the **Table of Contents**

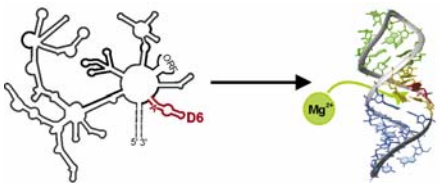

Group II intron ribozymes are self-splicing ribozymes. We present the first NMR structure of the branch domain 6 that includes the nucleophile for the first step of splicing. This adenosine is stacked within the helix in the presence and absence of Mg^{2+}, an essential cofactor for catalysis, which binds at the branch site. In addition, four more Mg^{2+} coordinate specifically within the branch domain.

Supplementary Material for

A Mg^{2+} Binding Site is Located in Close Neighborhood to the Stacked Branch-Adenosine in Domain 6 of a Self-Splicing Group II Intron Ribozyme

Michèle C. Erat,[a] Oliver Zerbe,[b] Thomas Fox,[a] and Roland K. O. Sigel*[a]

Running titles: (a) Domain 6 of a Group II Intron Ribozyme
(b) M. C. Erat et al.

---

[a] Prof. Dr. R. K. O. Sigel, Michèle C. Erat, Dr. T. Fox
Institute of Inorganic Chemistry, University of Zürich
Winterthurerstrasse 190
CH-8057 Zürich (Switzerland)
Fax: ++41-44-635 6802
Email: Roland.Sigel@aci.unizh.ch

[b] PD Dr. O. Zerbe
Institute of Organic Chemistry, University of Zürich
Winterthurerstrasse 190
CH-8057 Zürich (Switzerland)

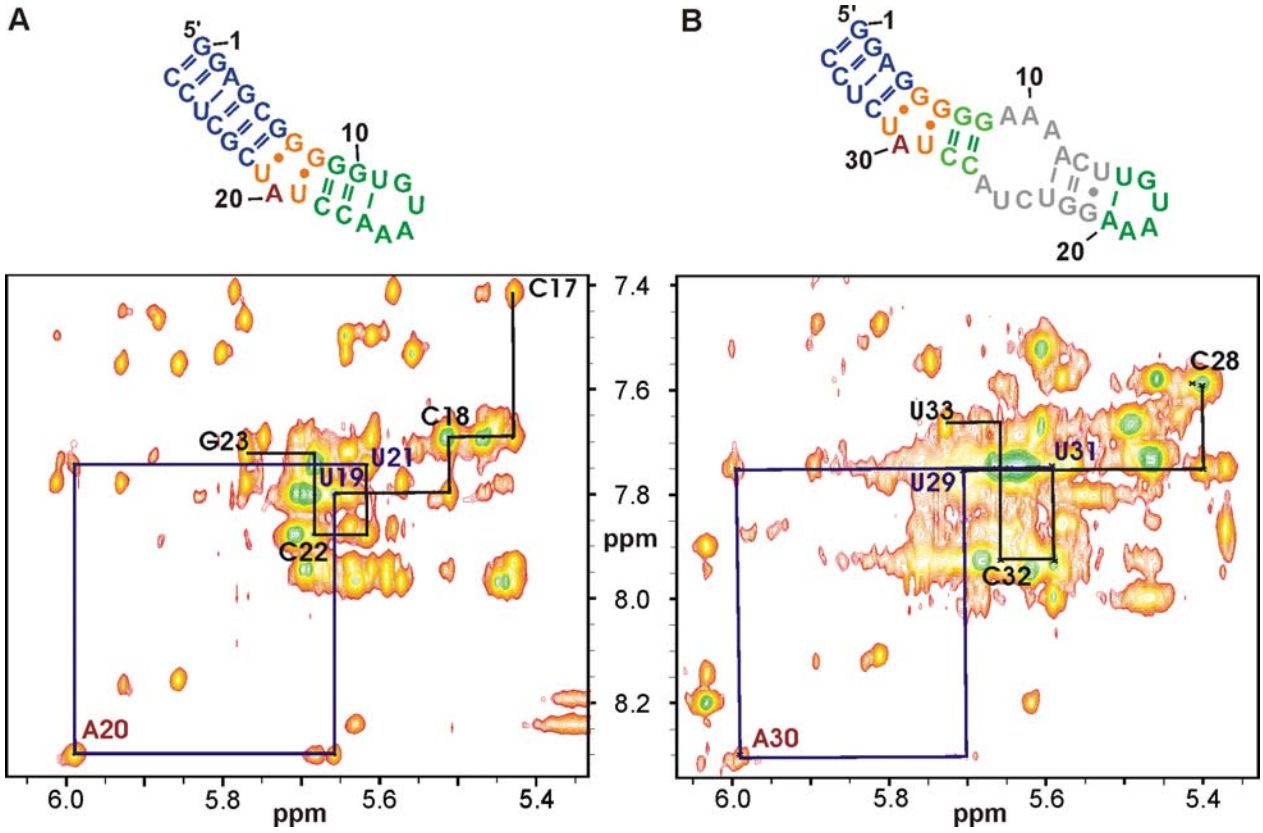

Supplementary Figure S1. Comparison of D6-27 and the full-length D6 from ai5γ. The corresponding parts of the [^{1}H,^{1}H]-NOESY spectra of D6-27 lacking the internal loop (A) and D6 with the internal loop in stem 2 (B) are shown (99.99% D_2O, pD 6.7, 100 mM KCl, 10 μM EDTA, 303 K). The sequential walk through the branch region including the branch adenosine with its 3'- and 5'-flanking nucleotides is indicated. The almost perfect agreement of the corresponding chemical shifts indicates an analogous structure in both D6 constructs.

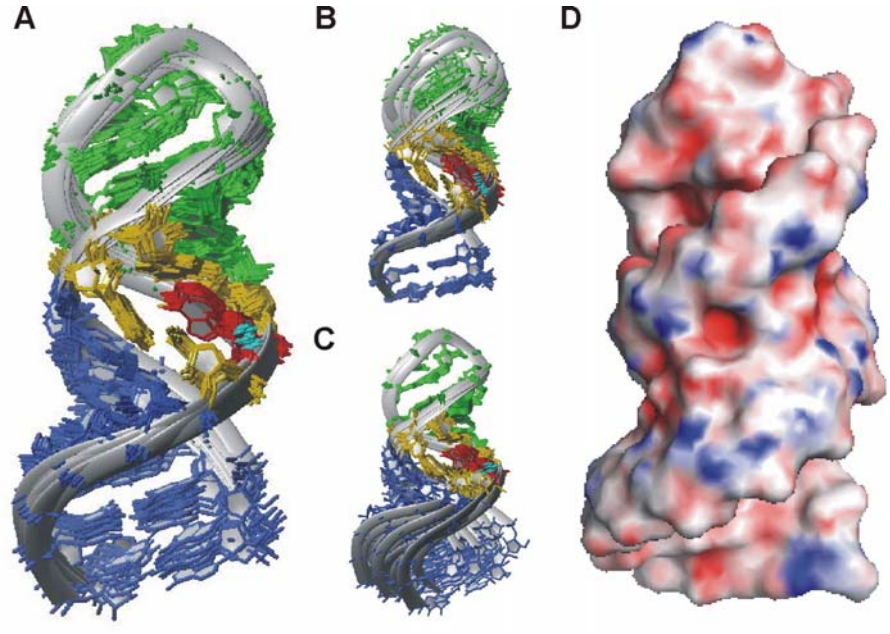

Supplementary Figure S2. D6-27 structure as determined by NMR. Helix 1 (nucleotides G1-G6, C22-C27) is colored in blue and helix 2 (nucleotides G9-C18) in green, the branch A20 in red, and the two flanking GU wobble pairs in gold. The nucleophile A20 2'-OH is shown in turquoise. (A) Superposition of all heavy atoms in D6-27 of the twenty lowest energy structures. (B) Superposition of the heavy atoms in stem 1 (nucleotides 1-6, and 22-27) of D6-27 of the twenty lowest energy structures. (C) Superposition of the heavy atoms in helix two of D6-27 (nucleotides 9-18) of the twenty lowest energy structures. (D) Calculated surface potential of D6-27. Red indicates negative, white neutral, and blue positive charge (red, –60; white –5; blue, 5 kTe^{-1}). D6-27 is shown in the same orientation as in (A) and Figure 1C. A highly negatively charged area in the minor groove can be seen at the Watson-Crick edge of A20.

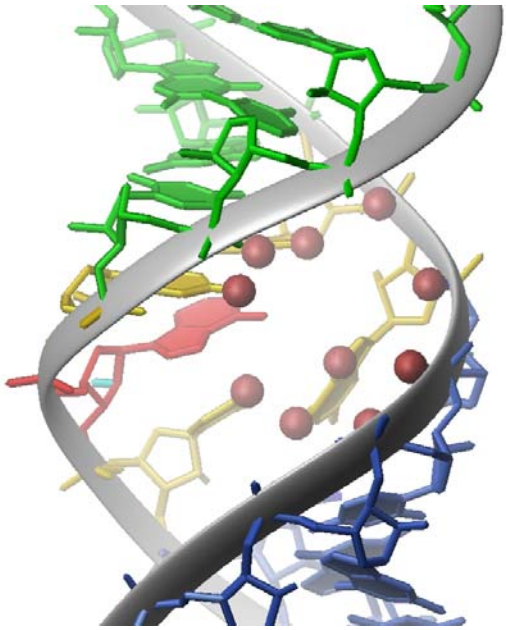

Supplementary Figure S3. Potential coordinating ligands for a metal ion bound to the major groove at the branch site are shown as red spheres. The combined oxygen atoms of the phosphate-diester groups, and the carbonyl oxygens of the GU wooble pairs (shown in orange) flanking the branch adenosine (shown in red) form a perfect binding pocket (see also Figure 1D).